

Electronic properties and ideal tensile strength of MoSe nanowires

Filipe J. Ribeiro, David J. Roundy, and Marvin L. Cohen

Department of Physics, University of California, Berkeley, California 94720

and Material Science Division, Lawrence Berkeley National Laboratory, Berkeley, California 94720

(Received 11 October 2001; published 22 March 2002)

Ab initio pseudopotential total energy calculations of MoSe nanowires were performed within the local density approximation. The $\text{Li}_2\text{Mo}_6\text{Se}_6$ crystal is composed of molecular chains, which can be separated from one another to form individual nanowires approximately 3 Å in diameter. In this study we consider three systems: the quasi-one-dimensional bulk crystal $\text{Li}_2\text{Mo}_6\text{Se}_6$, one isolated MoSe nanowire, and one isolated MoSe nanowire with Li adsorbates. The equilibrium structures and the electronic structures of the three systems were calculated and compared to each other. The calculated density of states of an isolated MoSe wire is compared with experimental tunneling spectroscopy measurements of the local density of states. The binding energy of a Li atom to an isolated wire was calculated and the effects of Li adsorption are discussed. In addition, the calculated value for the ideal tensile strength of a single MoSe nanowire is presented and compared with estimated values for carbon nanotubes.

DOI: 10.1103/PhysRevB.65.153401

PACS number(s): 73.22.-f, 61.46.+w, 62.25.+g, 71.20.-b

I. INTRODUCTION

Currently there is a great deal of interest in nanotubes and nanowires. In particular a large amount of experimental and theoretical research has been done on carbon nanotubes since their discovery in 1991 by Iijima.¹ The electronic properties of carbon nanotubes are known to be very sensitive to the structural configuration of the tube. Carbon nanotubes can be metallic or semiconducting depending on their chirality and diameter.² On the other hand, boron-nitride nanotubes are known to be large-gap semiconductors independent of their chirality and diameter.³ Even more recently, very small, subnanometer-diameter, MoS_2 single-walled nanotubes have been synthesized,⁴ which are remarkably similar in structure to the nanowires studied in this work, although they have a somewhat greater diameter.

Quasi-one-dimensional (quasi-1D) crystalline metallic structures with stoichiometry $M_2\text{Mo}_6X_6$ ($X = \text{Se, Te}$ and $M = \text{Li, Na}$) have been known since the work of Potel, and co-workers.⁵ Although these materials are synthesized in bulk crystalline form, their structures have a 1D character due to the presence of long molybdenum chains, along which the electrical conduction is supposed to occur. Previous studies^{6,7} have interpreted the electronic structure of bulk $\text{Ti}_2\text{Mo}_6\text{Se}_6$ in terms of quasi-1D metallic character. Dissolving $\text{Li}_2\text{Mo}_6\text{Se}_6$ in highly polar solvents yields bundles of MoSe chains and single isolated MoSe nanowires which can be deposited on a substrate.^{8,9} Recently, Venkataraman and Lieber¹⁰ used scanning tunneling microscopy (STM) to resolve and characterize the electronic structure of isolated MoSe nanowires. They found that bundles of MoSe chains and individual wires are metallic and the local density of states (LDOS) exhibits sharp peaks consistent with 1D Van Hove singularities. They also found that MoSe wires do not undergo a metal-insulator Peierls transition, remaining metallic down to at least 5 K.

Motivated by these recent experiments, *ab initio* pseudopotential calculations were performed on bulk $\text{Li}_2\text{Mo}_6\text{Se}_6$, single MoSe chain, and Li-doped single MoSe chain. The

lattice parameters, electronic band structures, charge density, and density of states were calculated for these systems.

II. METHOD

We performed *ab initio* pseudopotential total energy calculations within density functional theory (DFT) and the local density approximation¹¹ (LDA) using the Ceperley-Alder functional¹² for the exchange-correlation energy. The interaction of the valence electrons with the ionic cores is modeled by separable¹³ norm-conserving, Troullier-Martins¹⁴ pseudopotentials.

The total energy is calculated by a numerical integration over the Brillouin zone. For the bulk calculation we use a grid of $3 \times 3 \times 6$ k points. For the isolated wire there is no dispersion in the k_x and k_y directions, so we only need to sample 6 k points along the k_z axis. We expand the wave functions in plane waves¹⁵ up to a cutoff of 60 Ry. With these parameters, the total energy precision is better than 0.2 mRy/atom.

To find the equilibrium structure we relax the lattice parameters using a quasi-Newton method.¹⁶ The strained structure is obtained by fixing the c lattice constant and relaxing all other degrees of freedom.

III. STRUCTURE

The MoSe chains consist of an *ABAB* stacking of triangular Mo_3Se_3 elements as depicted in Fig. 1. Each Mo_3Se_3 element is an equilateral triangle with one Se atom at each vertex and one Mo atom between each pair of Se atoms. The relaxed distance between layers is 2.23 Å (or equivalently $c = 4.46$ Å), and the distance between two nearest Mo atoms within one layer is 2.77 Å; the separation between two Se atoms in the same layer is 5.21 Å.

In bulk $\text{Li}_2\text{Mo}_6\text{Se}_6$, MoSe chains are arranged in a triangular lattice with Li atoms in between the chains. For detailed plots of this structure and other related structures see Ref. 17. The lattice constants in the relaxed structure are a

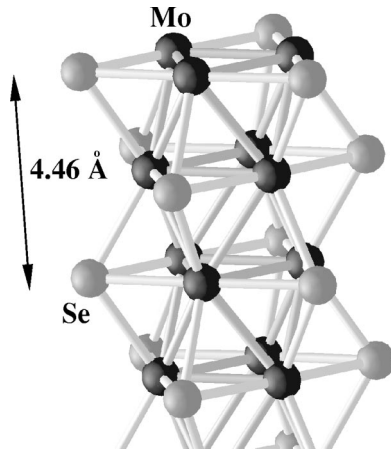


FIG. 1. A cut isolated MoSe chain. The chain is composed of an internal Mo chain surrounded by Se atoms.

$a=8.25$ Å and $c=4.51$ Å. The Mo-Mo distance is 2.71 Å, and the Se-Se distance is 5.24 Å. Compared to the isolated MoSe wire, the MoSe chains in crystalline form are stretched by 1%, the Mo-Mo distance is 2% shorter, and the Se atoms are 0.6% farther apart from each other.

We also calculate the adsorption energy of a Li on an isolated MoSe nanowire. To reduce the computational load, we chose a system with an inversion symmetry where two Li atoms approach the MoSe wire from opposite sides (Fig. 2). The Li binding site in our simulation was found to be at a distance of 4 Å from the axis of the MoSe chain, in the plane between two Mo_3Se_3 layers, and at equal distances from two Mo atoms of adjacent layers. Note that, in the bulk, the Li atoms are in the same plane of a Mo_3Se_3 unit and 4.76 Å away from the chain axis. The calculated binding energy of Li atom is about 2.5 eV.

IV. ELECTRONIC STRUCTURE

Bulk $\text{Li}_2\text{Mo}_6\text{Se}_6$ is known experimentally to be metallic.⁵ STM experiments¹⁰ have shown that isolated MoSe chains are also metallic and no Peierls transition occurs down to at least 5 K. Figures 3(a), 3(b), and 3(c) show the calculated band structures for an isolated wire, for an isolated wire plus two adsorbed Li atoms, and for a bulk crystal, respectively. The two wire systems are one dimensional and are periodic only in the direction of the wire axis. The bulk system is periodic in all three dimensions but its electronic structure has a strong 1D character. The band structure plot in Fig. 3(c) shows that the energy band dispersion is stronger in the Γ -A direction—parallel to the wire axis—than in the A-L direction. This is because bulk $\text{Li}_2\text{Mo}_6\text{Se}_6$ is a periodic arrangement on MoSe wires which are relatively far apart from each other. All three systems are seen to be metallic, in agreement with experiment. There are 72 valence electrons per unit cell in an isolated MoSe wire. In the bulk crystal and the isolated wire plus adsorbates there are 74 valence electrons per unit cell. The two Li atoms donate their electrons to the MoSe chain, raising the Fermi level and leaving the band structure relatively unperturbed. The low-energy bands be-

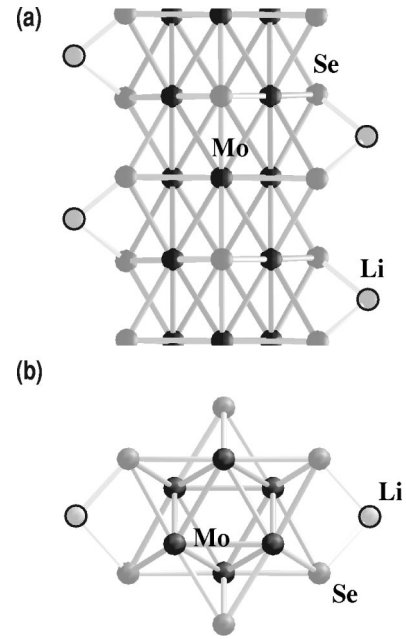


FIG. 2. (a) Side and (b) top views of a single MoSe nanowire with two adsorbed Li atoms per unit cell.

tween -12 eV and -15 eV common to the three systems correspond to Se s -like states.

In the band structure of the isolated wire [Fig. 3(a)], there are three bands which cross the Fermi level. The plot of the electronic charge density in an isolated MoSe wire for the occupied states close to the Fermi energy [Fig. 3(d)] shows that the conduction channels are essentially localized around the Mo atoms. The band with the small hole pocket at the Γ point is doubly degenerate. Therefore, on a single MoSe wire there are four conduction channels, and the quantum conductance (which would be the conductance in the ballistic limit) of the wire is predicted to be $4 G_0$, where G_0 is the quantum conductance constant $2e^2/h$. Because the doubly degenerate band is flat and close to the Fermi level, the quantum conductance will be rather sensitive to the electronic doping level. Increasing the number of electrons of the system will raise the Fermi level. A doping of the order of 0.3 electrons per unit cell is enough to fully occupy the doubly degenerate band and reduce the number of conduction channels to 2. Further doping will lead to the occupancy of the next band, leaving only one conduction channel. On the other hand, doping with acceptors will lower the Fermi level which might increase the quantum conductance.

For a doping level of 2 Li atoms per unit cell ($\text{Li}_2\text{Mo}_6\text{Se}_6$) the stoichiometry of the wire corresponds to the stoichiometry of the bulk crystal and the Fermi levels should align as shown in Figs. 3(b) and 3(c). The main features of the band structure are the same as in the isolated MoSe wire, consistent with the picture of Li acting as a donor atom. It is expected that other alkali atoms will also transfer charge to the wire and the effects on the band structure and Fermi level will be similar.

Figures 4(a) and 4(b) show the measured normalized conductance¹⁰—which is proportional to the LDOS—for MoSe wires deposited on Au(111) and highly oriented pyro-

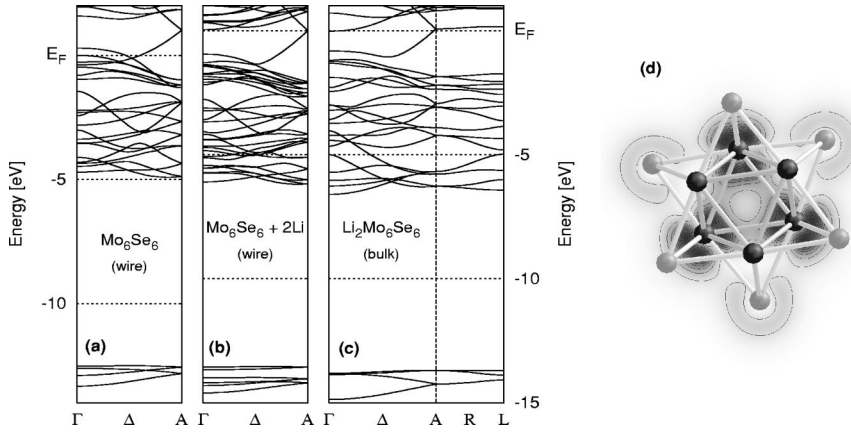


FIG. 3. Band structures and charge density plot: (a) band structure of an isolated MoSe nanowire, (b) band structure of a MoSe wire with two Li adsorbates, (c) band structure of bulk $\text{Li}_2\text{Mo}_6\text{Se}_6$, and (d) electronic charge density of states with energy close to the Fermi level, plotted on the plane of a Mo_3Se_3 layer.

lytic graphite (HOPG), respectively. Figure 4(c) shows the calculated total DOS of an isolated MoSe wire. It is important to note that what is measured is the local density of states, not the total density of states, which is calculated. Nevertheless, because there is no real distinction between surface and bulk atoms in this system, it is still meaningful to compare the LDOS with the total DOS. A common feature of the three plots is the flat region of low DOS above the Fermi level which extends for more than 1 eV. This is associated with the highly dispersive band at and above E_F [see the band structure in Fig. 3(a)]. In the experiment, the first strong Van Hove singularity above the Fermi level occurs at about 1.2 V slightly lower than the calculated value of 1.5 V. Charge transfer from the substrate may account for this difference. In fact, shifting up E_F in the theoretical plot by roughly 0.4 eV we can almost map the Van Hove singularities between Figs. 4(a) and 4(c). This shift would raise the Fermi level beyond the first Van Hove singularity above E_F . By taking into account the band structure of the isolated wire one can estimate that the amount of charge necessary for this shift is roughly one electron per Mo_6Se_6 unit cell.

V. IDEAL STRENGTH

The total energy and axial restoring force for different values of strain were calculated. For small values of strain we expect plastic deformation, i.e., reversible, linear restoring force as a function of strain according to Hooke's law. For an isolated MoSe nanowire our results show that the force constant is 165 nN. Young's modulus is not a well-defined quantity for nanowires because of the difficulty in defining the cross-sectional area. If one defines the area of the wire as the area of a circle of radius equal to the distance of the Se atoms to the axis of the wire ($A = 0.29 \text{ nm}^2$), a value for Young's modulus of approximately 570 GPa is found.

As we increase the strain, the force will progressively deviate from a linear regime and eventually will reach a maximum value. This maximum force is the *ideal tensile strength*. It represents the highest force sustainable by the wire in an ideal situation where there is no symmetry breaking of the structure. In reality one should expect the wire to break down for forces much smaller than the maximum force due to defects or inhomogeneities of the stress. Nevertheless,

the ideal tensile strength is an interesting quantity because it establishes an upper limit on the strength. To calculate the force as a function of strain ϵ we set the axial lattice constant c to $c_0(1 + \epsilon)$ and relax all the atomic degrees of freedom. Relaxation is an important step of the calculation because, for each value of the strain, the correct stress corresponds to the ground state of the constrained system.

In Fig. 5 we plot the force as a function of strain. The maximum force is 15.5 nN at a strain of 19%. It is interesting to compare this value with ideal strength values for carbon nanotubes. A nanotube can be viewed as a graphene sheet rolled into a tubular shape. For similar calculations on the ideal tensile strength of graphene sheets, there are two directions of particular interest. One corresponds to the axis of an *armchair* nanotube and the other corresponds to the axis of a *zigzag* nanotube. Straining along the armchair direction we find an ideal strength of 77 nN/nm and straining along the zigzag direction we get an ideal strength of 71 nN/nm. The units are force per unit length (nN/nm) because graphene sheets are two-dimensional objects. Since a single-wall nanotube is a rolled-up graphene sheet, one can estimate its ideal strength by multiplying the ideal strength of graphene by the circumference of the tube. The smaller the circumference, the weaker the tube will be. Typical tubes that can be synthesized are around 1 nm in diameter, which corresponds to a circumference of roughly 3 nm. Therefore the ideal strength of a typical nanotube is approximately $3 \text{ nm} \times 71 \text{ nN/nm} \sim 200 \text{ nN}$. We recall the value of 15.5 nN obtained for the strength of a MoSe nanowire and conclude that the ideal tensile strength of MoSe nanowires is more than one order of magnitude smaller than the ideal tensile strength of single-wall carbon nanotubes.

VI. CONCLUSION

We describe first-principles total energy calculations for MoSe-nanowire-related systems. The band structures for the studied systems reveal that they are all metallic. Li atoms bind to isolated MoSe wires at a site between two Mo_3Se_3 layers, and the binding energy is roughly 2.5 eV per Li atom. The band structures of the doped and undoped wires exhibit striking similarities, indicating that Li acts mainly as an electron donor and the Fermi level is raised according to the Li concentration. This suggests that other alkali atoms would

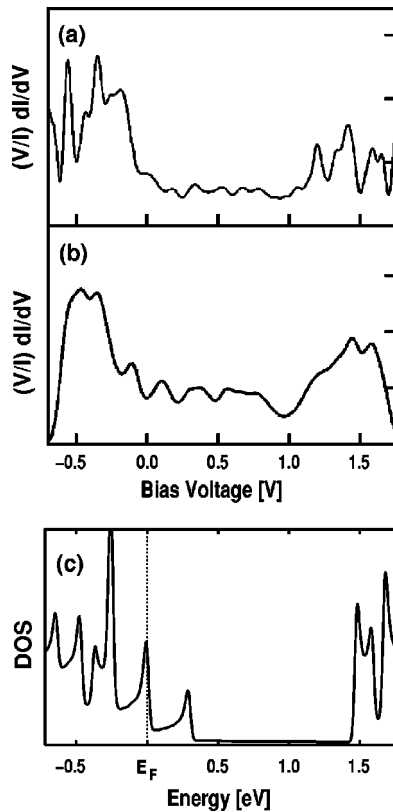


FIG. 4. Experimental normalized conductance in (a) Au substrate and (b) graphite substrate. The experimental data are taken from Ref. 10. (c) Calculated total density of states convoluted with a Gaussian of 0.02 eV of width.

also behave as donors. Raising or lowering the Fermi level of a MoSe wire by doping has the effect of changing the number of conduction channels of the system. Even at high concentrations of donors the MoSe nanowires remain metallic. Because all MoSe nanowires are structurally identical, they are all metallic and they all have the same electronic structure. This is an advantage over carbon nanotubes, where the

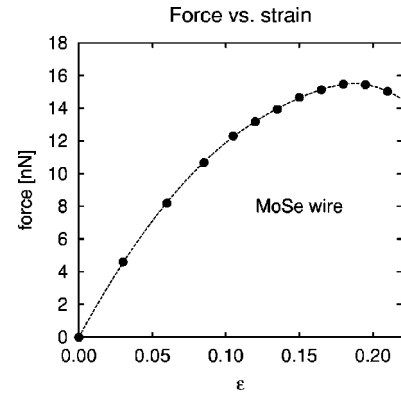


FIG. 5. Plot of the restoring force as a function of strain for an isolated MoSe nanowire. The dotted line is a fit to the calculated points.

electronic properties depend on radius and chirality which are difficult to control.

We also conclude that the ideal strength of MoSe nanowires under tensile strain is 15.5 nN which is roughly one order of magnitude lower than the ideal tensile strength of a typical carbon nanotube. As a final remark we stress that, although MoSe nanowires are not as strong as carbon nanotubes, their easily controlled electronic properties present advantages for electronic applications.

ACKNOWLEDGMENTS

We would like to thank Seung-Hoon Jhi for helpful discussions. This work was supported by the National Science Foundation under Grant No. DMR-0087088 and by the Office of Energy Research, Office of Basic Energy Sciences, Materials Sciences Division of the U.S. Department of Energy under Contract No. DE-AC03-76SF00098. One of the authors (F.J.R.) was supported by FCT PRAXIS/BD/13465/97. Computational Resources were provided by NCSA and by NERSC.

- ¹S. Iijima, *Nature (London)* **56**, 354 (1991).
- ²N. Hamada, S.I. Sawada, and A. Oshiyama, *Phys. Rev. Lett.* **68**, 1579 (1992).
- ³N.G. Chopra *et al.*, *Science* **269**, 966 (1995).
- ⁴M. Remskar *et al.*, *Science* **292**, 479 (2001).
- ⁵M. Potel *et al.*, *J. Solid State Chem.* **35**, 286 (1980).
- ⁶T. Hughbanks and R. Hoffman, *Inorg. Chem.* **21**, 3578 (1982).
- ⁷T. Hughbanks and R. Hoffman, *J. Am. Chem. Soc.* **105**, 1150 (1983).
- ⁸J.M. Tarascon *et al.*, *J. Solid State Chem.* **58**, 290 (1985).
- ⁹M.D. Hornbostel *et al.*, *Nanotechnology* **6**, 87 (1995).
- ¹⁰L. Venkataraman and C.M. Lieber, *Phys. Rev. Lett.* **83**, 5334

- (1999).
- ¹¹M.L. Cohen, *Phys. Scr.* **T1**, 5 (1982).
- ¹²D.M. Ceperley and B.J. Alder, *Phys. Rev. Lett.* **45**, 566 (1980).
- ¹³L. Kleinman and D.M. Bylander, *Phys. Rev. Lett.* **48**, 1425 (1982).
- ¹⁴J.L. Martins, N. Troullier, and S.-H. Wei, *Phys. Rev. B* **43**, 2213 (1991).
- ¹⁵J. Ihm, A. Zunger, and M.L. Cohen, *J. Phys. C* **12**, 4409 (1979).
- ¹⁶B.G. Pfrommer *et al.*, *J. Comput. Phys.* **131**, 233 (1997).
- ¹⁷J.M. Tarascon, G.W. Hull, and F.J. DiSalvo, *Mater. Res. Bull.* **19**, 915 (1984).